Physical Properties of Highly Concentrated Barium Sulfate Contrast Agent Used in Gastric Cancer Screening

東北大医保健学科紀要　**23**(2)：83～93，2014

Original Paper

Physical Properties of Highly Concentrated Barium Sulfate Contrast Agent Used in Gastric Cancer Screening

Akihito USUI[1], Yoshiyuki HOSOKAI[1], Yusuke KAWASUMI[2], Haruo SAITO[1] and Shiro KAMBE[3]

[1]*Diagnostic Image Analysis, Tohoku University Graduate School of Medicine*
[2]*Clinical Imaging, Tohoku University Graduate School of Medicine*
[3]*Department of Chemistry and Chemical Engineering, Yamagata University*

胃がん検診用高濃度硫酸バリウムの物理特性

臼井章仁[1]，細貝良行[1]，川住祐介[2]，齋藤春夫[1]，神戸士郎[3]

[1]東北大学大学院医学系研究科　画像解析学分野
[2]東北大学大学院医学系研究科　画像診断学分野
[3]山形大学工学部　物質科学工学科

Key words : Highly concentrated barium sulfate, Contrast agent, Gastric cancer screening, Particle size distribution, Viscosity, Suspension rheology

A highly concentrated barium sulfate contrast agent is currently used for gastric cancer screening in many medical institutions in Japan. The required viscosity of a solution depends on the particle size distribution of the agent. Barium sulfate contrast agent is composed of large particles and is referred to as a high-density product ; it is a low-viscosity solution for maximum coverage of the gastric mucosa. The particle size distribution, viscosity, and concentration of barium sulfate are all inter-related factors of this high-density product. We confirmed by using scanning electron microscopy and laser diffraction spectrometry that there are barium sulfate contrast agent high-density products on the market that contain both small, fine particles as well as large, coarse, angular particles. The fine particles were approximately 1.0-3.0 μm in size and the coarse particles measured approximately 15 μm in size. The swallowing action causes the load of shear rate of 10 s^{-1} to the intralaryngeal bolus. The viscosity of the barium sulfate contrast agent appeared to decrease following the act of swallowing, thus enabling easy swallowing, whereas the viscosity at a different shear rate increased over time and exhibited a dilatant behavior. The ability of the suspension to coat the gastric mucosa by dilatant effect was maintained during changes in body position and during the resting state. A thoroughly mixed high-density-product suspension maintains an adequate viscosity and demonstrates a high level of mucosal detail.

1. Introduction

The gastrointestinal tract is a succession of hollow organs. It is generally investigated by use of X-ray imaging, which requires the use of a contrast agent introduced orally or via the rectum. Historically, the first studies of gastrointestinal contrast agents involved various substances, including bismuth subnitrate. However, bismuth subnitrate occasionally induced nitrite poisoning. In 1910, the

routine use of barium sulfate was proposed for gastrointestinal examination because of its lack of toxicity[1]. Henceforth, this substance has remained the agent of choice.

A highly concentrated barium-sulfate contrast agent has been developed and is currently used for gastric cancer screening in numerous medical institutions[2,3]. Barium sulfate exhibits advantageous characteristics, such as insolubility in water and acids, stability, a high atomic number, and low cost[4]. Among these advantages, the high atomic number of the substance exhibits a large X-ray absorption coefficient and demonstrates high contrast on a radiograph. Currently, this contrast agent is also the principal substance used in gastrointestinal fluoroscopic imaging studies, for both the repletion and the double-contrast method.

Currently, a double-contrast method using both highly concentrated barium sulfate and a gas-producing agent is commonly used in routine gastric cancer screening examination for achieving fine mucosal detail[5,6]. The highly concentrated barium sulfate agent consists of a distribution of particle sizes. The particle size influences the sedimentation rate and viscosity of the suspension. The small particles of the barium-sulfate contrast agent induce a high viscosity because of larger surface area and interaction[4]. Conversely, the large particles give rise to a lower viscosity because of smaller surface area and interaction. The final viscosity achieved depends on the particle size distribution of the agent. This contrast agent, which involves large particles, is a high-density (HD) product that has a low viscosity for nearly ideal coverage of gastric mucosa. Our aim in this study was to evaluate the particle size distribution and viscoelasticity of HD barium agents currently on the market in comparison with previous products that are no longer available.

2. Materials and Methods

2.1 Materials

Six different barium-sulfate powder samples were prepared. These were BarytgenHD and BarytesterA240 (Fushimi Pharmaceutical Co., Ltd. Kagawa, Japan), the on-market type and off-market type of NeobalginHD (Kaigen Co., Ltd. Osaka, Japan), and the on-market type and off-market type of Baliconmeal (Horii Pharmaceutical Ind., Ltd. Osaka, Japan) (Table 1). All samples contain mainly barium sulfate powder and some functional excipients selected by manufacturers.

To evaluate the crystallographic properties of barium sulfate, we investigated the constituent elements and averaged the crystallite components by using X-ray powder diffraction (XRD). To evaluate the morphology, we used a scanning electron microscope (SEM). To evaluate the particle size distribution of a barium sulfate suspension in water, we used laser diffraction spectrometry (LDS). Finally, to evaluate the rheology, we measured the flow curve and dynamic viscoelasticity by using a modular rheometer.

2.2 X-ray powder diffraction measurement

The XRD samples were prepared on glass slides, and measurements were performed with RINT2000 (Rigaku, Tokyo, Japan). All powder samples were irradiated with copper K_α radiation. The X-ray tube voltage and current were set at 40 kV and 20 mA, respectively. Diffraction patterns were recorded from $2\theta = 3^\circ$ to 60° at a scan rate of 4°/min. A crystal is a given atomic pattern repeated in three dimensions. The unit cell is defined as constituting a basis for the crystal lattice. The crystallographic planes are characterized by three integers, referred to as the Miller indices. The Joint committee in powder diffraction standards (JCPDS) database is the standard database for XRD data, including that Miller indices and peak intensities, for natural and synthetic materials. Unknown crystallographic sub-

Table 1. Barium sulfate contrast agents used for our experimental purposes.

Product	Manufacturer	Commercially available
BarytgenHD	Fushimi	Yes
BarytesterA240	Fushimi	Yes
NeoBalginHD (previous type)	Kaigen	No
NeoBalginHD (later type)	Kaigen	Yes
BaliconMeal (previous type)	Horii	No
BaliconMeal (later type)	Horii	Yes

stances are commonly identified by use of the XRD measurement to compare diffraction data against the JCPDS database. Next, the average crystallite size was calculated from the XRD patterns obtained by use of the Debye-Scherrer formula[7] ;

$$D = \frac{k\lambda}{\beta \cos\theta}, \qquad (1)$$

in which D is the crystallite size in nanometers (length of normal direction of lattice plane represented by the Miller index), Scherrer factor $k = 0.89$, X-ray wavelength $\lambda = 0.154$ nm, β is half maximum full-width in radians, and θ is Bragg angle in radians. However, for the Baliconmeal currently on the market, this was not measured.

2.3 Scanning electron microscopy

FE-SEM JSM-6330F (JEOL Ltd, Tokyo, Japan) was used for obtaining images of particles at a 20 kV acceleration voltage. We observed and analyzed the SEM images at magnifications of 1,000-5,000 fold.

2.4 Laser diffraction spectrometry

LDS utilizes the diffraction pattern of a laser beam that has passed through a substance ; particle size is measured by analysis of the intensity of light scattered by a particle because it is directly proportional to the size of the particle. The LDS method measures the particle size distribution and requires that the particles be in a dispersed state. All samples were prepared at a barium sulfate concentration of 200 w/v% (percentage weight in volume) with water. We obtained two types of particle size distributions, which represent the cumulative distribution and frequency of distribution of barium sulfate suspensions, by using a laser diffraction particle size analyzer (SALD-7000, Shimadzu Corporation, Kyoto, Japan). The slope of the cumulative distribution cited at any point represents the rate of frequency at that point. The local maximum rate of frequency corresponds to the inflection point of the cumulative distribution[8]. Next, we analyzed the median particle diameter (d50) and the mean particle diameter. The d50 corresponds to 50% of a cumulative distribution and indicates that half of the particles are smaller (or larger) than the median. The mean particle diameter, d_{mean}, is given as follows[9] :

$$d_{\mathrm{mean}} = \frac{\sum n_j d_j}{\sum n_j}, \qquad (2)$$

in which n_j is the number of particles of size d_j and the sum of n_j represents the size of all measured particles. All samples potentially include many irregular particles. An irregular particle exhibits a certain surface area in which an equivalent sphere could be chosen that exhibits an identical surface area. The definition of the equivalent spherical diameter is based on this concept of identical surface area. The surface area of a sphere, with diameter d, is $\pi^2 d^2$.

2.5 Rheologic measurements

Rheologic measurements for BarytesterA240 (200 w/v%) were obtained at room temperature by use of

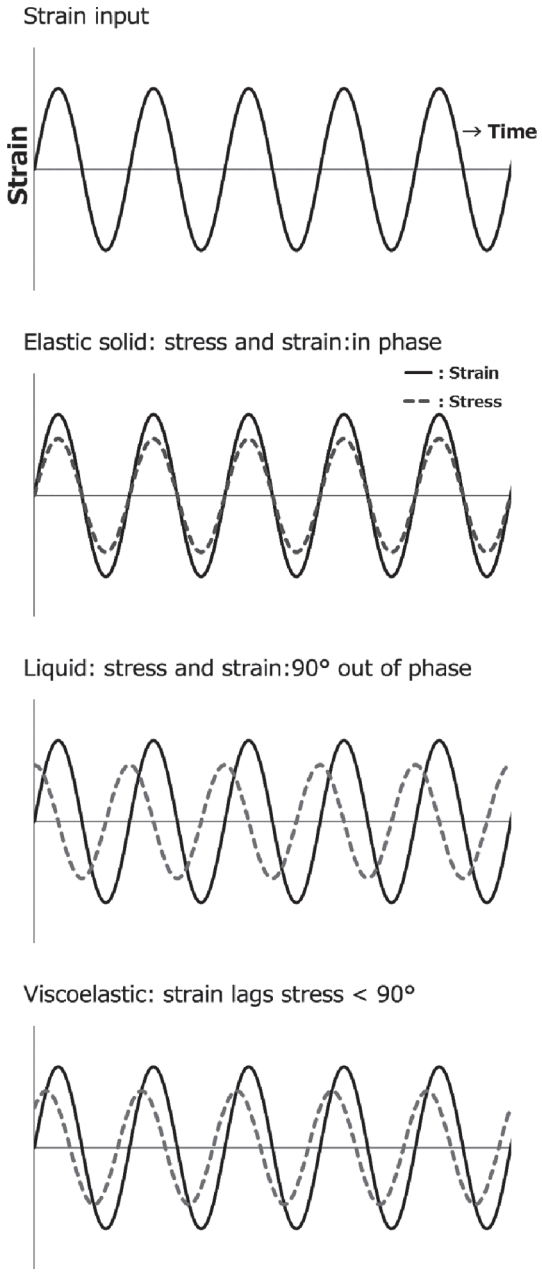

Figure 1. Stress vs. strain response of a Newtonian fluid, a Hookean elastic solid, and a viscoelastic material in a dynamic test.

a modular rheometer (Physica MCR301, Anton Paar GmbH, Graz, Austria). Rheology is the study of flow ; we measured the flow curve and the dynamic viscoelasticity. A flow curve is a graphic representation of the behavior of flowing materials that depicts the relationship between stress and shear rate. We obtained the flow curve of the prepared barium sulfate suspension.

Dynamic viscoelastic behavior can be measured by the application of an oscillatory stress of small amplitude. The shear stress applied produces a corresponding strain in the material. The storage modulus G' describes the elasticity of a material. If the material behaves elastically or in a highly structured manner, like a gel, G' has a value of unity. If G' is zero, the material behaves as fully viscous and has no inner structure. The loss modulus G'' refers to the viscous properties and quantifies the degree of energy dissipation. If G'' is zero, the material behaves as a Hookean elastic material (Fig. 1). This is related to the oscillation frequency ω and phase angle ωt by

$$G^*(\omega) = G'(\omega) + iG''(\omega) = G^*\cos\omega t + iG^*\sin\omega t, \tag{3}$$

in which G^* is the complex modulus, i is the square root of -1, and t is time[10]. The complex number G^* is an ordered pair of real numbers where G' is the real part and G'' the imaginary part (Fig. 2). The absolute value of the complex viscosity $|G^*|$, the storage modulus G' and the loss modulus G'' are represented in pressure unit. They are Pascal (symbol : Pa), which is defined as 1 Nm^{-1}. For a Newtonian fluid, $\omega t = \pi/2$, and for a Hookean elastic material, $\omega t = 0$, whereas viscoelastic materials exhibit a phase angle between these two limits. The complex viscosity η^* is defined as

$$\eta^*(\omega) = \eta'(\omega) - i\eta''(\omega) = \eta^*\cos\omega t - i\eta^*\sin\omega t \tag{4}$$

$$\eta' = \frac{G''}{\omega} \tag{5}$$

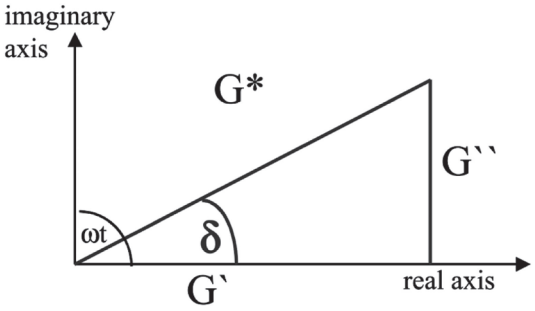

Figure 2. Plot of the complex modulus G^*. The horizontal real axis indicates the elastic or storage modulus, and the vertical imaginary axis indicates the viscous or loss modulus. ωt is the phase angle.

$$\eta'' = \frac{G'}{\omega}, \qquad (6)$$

in which η' represents the dynamic viscosity (viscous component) and η'' represents a parameter related to the storage modulus (elastic component). The complex viscosity function is equal to the difference between the dynamic viscosity η' and η''. The viscosity is represented in SI units. They are Pascal-seconds (symbol : Pas), which is defined as 1 $kgm^{-1}s^{-1}$. For dynamic rheologic measurements, we performed frequency sweep studies in which G' and G'' are determined as a function of the angular frequency ω at room temperature. In Japanese, G' is called "Neba-neba" and G'' is called "Sara-sara".

3. Results and Discussion

3.1 Composition and crystallite size

The XRD patterns of BarytesterA240, BarytgenHD, NoebalginHD (on-market type), NeobalginHD (previous type), and Baliconmeal (previous type) can be seen in Figure 3. The XRD patterns shown in Figure 3 were obtained by comparison of the data with patterns in a JCPDS database. The peaks assigned to barium sulfate (JCPDS database No. 24-1035) demonstrated that the composition of the material was indeed barium sulfate. Based on the results of XRD patterns, we calculated the averaged crystallite size by using Eq. (1). As shown in Table 2, particle sizes ranged from 32 to 47 nm. We demonstrated that particles of barium sulfate essentially consist of tens of nanosized crystallites.

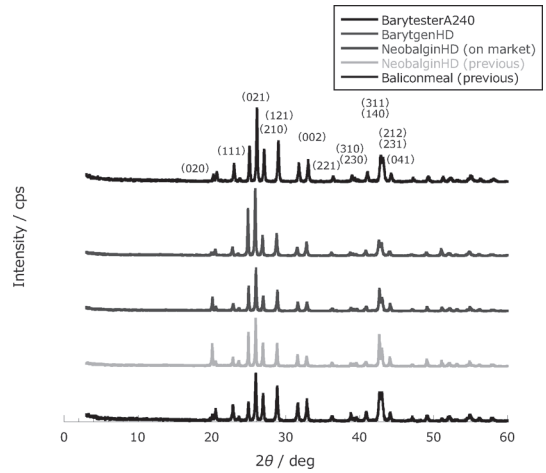

Figure 3. X-ray powder diffraction (XRD) patterns of barium-sulfate contrast agents. In this graph, the horizontal axis shows the diffraction angle 2θ, and the vertical axis shows X-ray intensity in arbitrary units. These patterns are identified the index of each peaks.

Table 2. Crystallite size calculated from the XRD patterns obtained by use of the Debye-Scherrer formula.

Products	Crystallite size [nm]
BaliconMeal (previous)	32 (27-39)
BarytesterA240	37 (24-47)
BarytgenHD	41 (28-53)
NeobalginHD (previous)	44 (32-55)
NeobalginHD (on-market)	47 (33-57)

3.2 Particle size

The SEM images of BarytgenHD, BarytesterA240, NeobalginHD (previous type), NoebalginHD (on-market type), Baliconmeal (previous type), and Baliconmeal (on-market type) are shown in Figures 4-1 through 4-3. We observed that the on-market type of barium sulfate powder contained a high proportion of particles measuring above 10 μm,

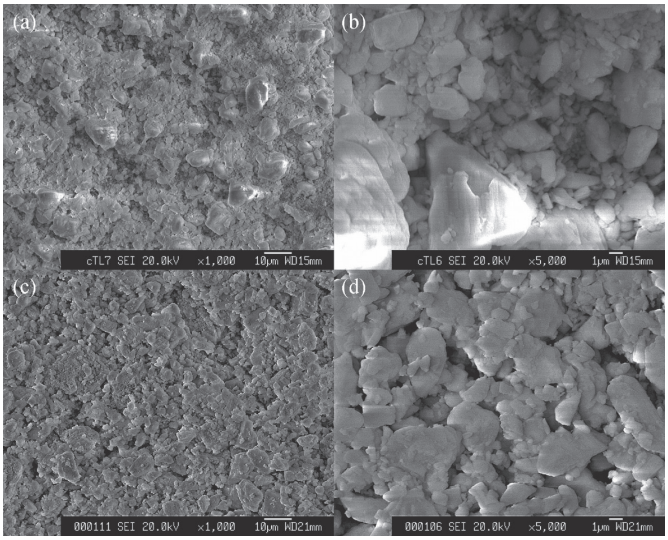

Figure 4-1. Scanning electron micrographs of barium-sulfate contrast agents. In the 1,000-fold magnified image, the bar represents 10 μm, at 5,000-fold magnification, the bar represents 1 μm.
(a) BarytgenHD : image at 1,000-fold magnification.
(b) BarytgenHD : image at 5,000-fold magnification.
(c) BarytesterA240 : image at 1,000-fold magnification.
(d) BarytesterA240 : image at 5,000-fold magnification.

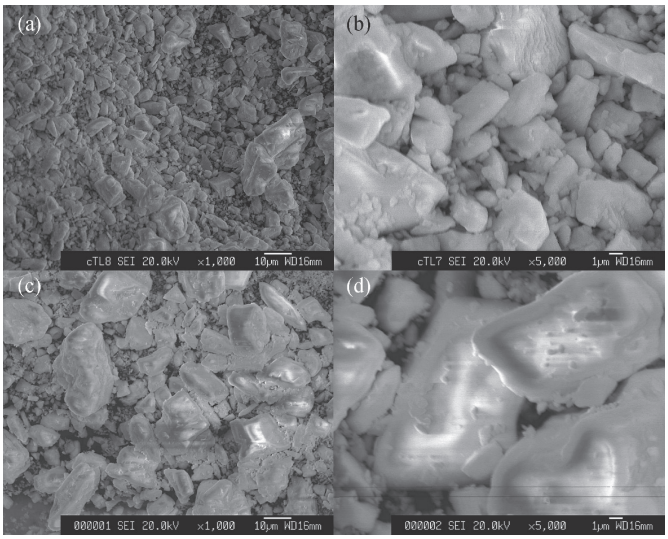

Figure 4-2. Scanning electron micrographs of barium-sulfate contrast agents.
(a) Baliconmeal (previous type) : image at 1,000-fold magnification.
(b) Baliconmeal (previous type) : image at 5,000-fold magnification.
(c) Baliconmeal (on-market type) : image at 1,000-fold magnification.
(d) Baliconmeal (on-market type) : image at 5,000-fold magnification.

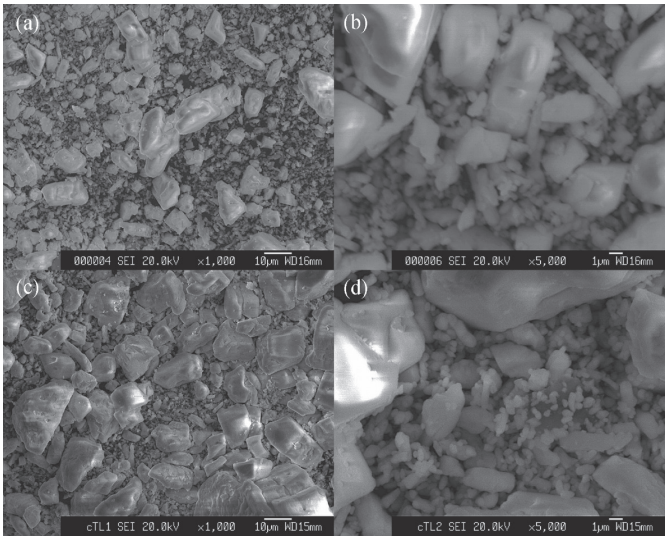

Figure 4-3. Scanning electron micrographs of barium-sulfate contrast agents.
(a) NeobalginHD (previous type) : image at 1,000-fold magnification.
(b) NeobalginHD (previous type) : image at 5,000-fold magnification.
(c) NeobalginHD (on-market type) : image at 1,000-fold magnification.
(d) NeobalginHD (on-market type) : image at 5,000-fold magnification.

and among the large particles with an angular shape the particle measurements reached approximately 30 μm. Among the products, it was observed that Baliconmeals were composed of nearly all angular particles. In particular, NeobalginHDs were clearly composed of small, rounded particles measuring approximately 1 μm and angular particles that ranged in size from approximately 10 to 30 μm. The angular particles and those with small, rounded shapes were considered coarse particles and fine particles, respectively. The coarse particles are extracted from mines and treated by physical and chemical processes to achieve the specifications of the relevant pharmacopoeia. The fine particles are obtained by precipitation of other barium salts with sulfuric acid, and they are washed to ensure purity[4].

The cumulative distribution of barium sulfate suspensions obtained by LDS is shown in Figure 5. The d50 of more recent products has tended to be composed of a majority of particles measuring more than 7 μm, compared with previous, off-market

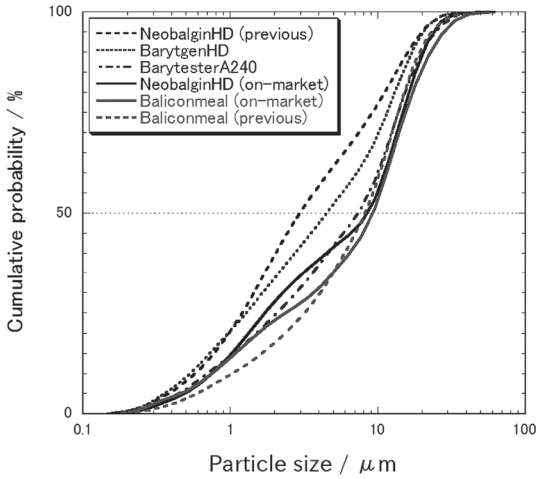

Figure 5. Cumulative distributions of barium sulfate contrast agents. The horizontal logarithmic axis shows particle size, and the vertical axis shows cumulative probability. The median diameter size (d50) corresponds to 50% on the cumulative distribution and indicates that half of the particles have sizes smaller (or larger) than the median.

Table 3. Median diameter size obtained from the cumulative distribution.

Products	Median diameter, d50 [μm]
NeoBalginHD (previous)	3.0
BarytgenHD	4.5
BarytesterA240	7.3
BaliconMeal (previous)	8.2
NeoBalginHD (on-market)	8.4
BaliconMeal (on-market)	9.2

Table 4. Mean diameter size obtained from the frequency distribution.

Products	Mean diameter size, d_{mean} [μm]
NeoBalginHD (previous)	6.7
BarytgenHD	7.9
BarytesterA240	10.1
NeoBalginHD (on-market)	10.4
BaliconMeal (previous)	10.5
BaliconMeal (on-market)	11.7

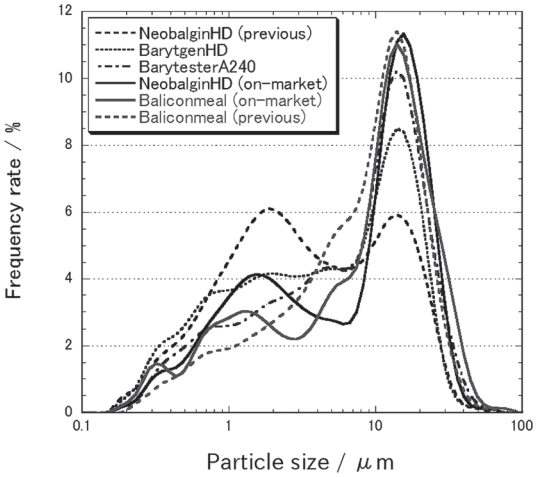

Figure 6. Frequency distributions of barium sulfate contrast agents. The horizontal logarithmic axis shows particle size, and the vertical axis shows the frequency rate.

products (Table 3).

The distribution of the barium sulfate suspension is shown in Figure 6. All samples indicated that the peak occurred at a particle size of approximately 15 μm. The previous type of Baliconmeal exhibited a unimodal distribution with just this one peak, in the manner of a Gaussian distribution. BarytgenHD and BarytesterA240 exhibited this one peak, as well as a decrease in particle size in correlation with the frequency rate, resulting in a larger peak height for BarytesterA240 in comparison with BarytgenHD. NeobalginHDs clearly exhibited a bimodal distribution, with two peaks at approximately 15 μm, and had a range of 1.0 to 3.0 μm. The particles ranging from 1.0 to 3.0 μm were considered fine particles, whereas the particles greater than approximately 10 μm were considered coarse particles. The peak that was representative of the frequency of the distribution corresponded closely with the morphologic observations by the scanning electron micrographs of fine and coarse particles. We found that more recent on-market products contained the highest percentage of large, coarse particles because of the presence of the largest frequency of the distribution peak at a particle size of approximately 15 μm.

Next, we obtained the mean diameter, calculated by use of Eq. (2), resulting in a range of 6.7 to 11.7 μm (Table 4). The mean particle diameter of recent products tended to be greater than 10 μm. Therefore, the viscosity of this product is expected to decrease, because of the larger particle size gives rise to smaller particulate total surface and interaction.

3.3 Flow curve and dynamic viscoelasticity

The flow curve of the barium sulfate suspension (BarytesterA240, 200 w/v%) did not demonstrate direct linearity between shear stress and shear rate, as shown in Figure 7. This indicates that this suspension behaves as a non-Newtonian fluid. The flow of some materials does not commence until they reach a threshold value of stress, called a yield stress. The yield stress of this suspension is very small, as shown in Figure 7. Because a yield stress is attributed to a deformity in the inter-particle network of binding forces, this result indicates that

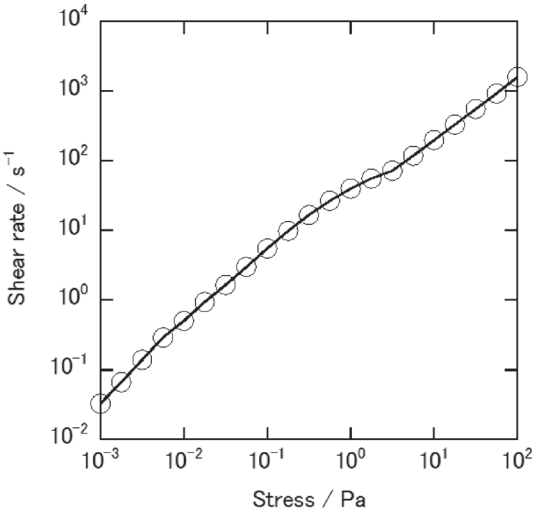

Figure 7. Flow curve of barium-sulfate contrast agent (BarytesterA240, 200 w/v%). The horizontal logarithmic axis shows shear stress, and the vertical logarithmic axis shows shear strain rate.

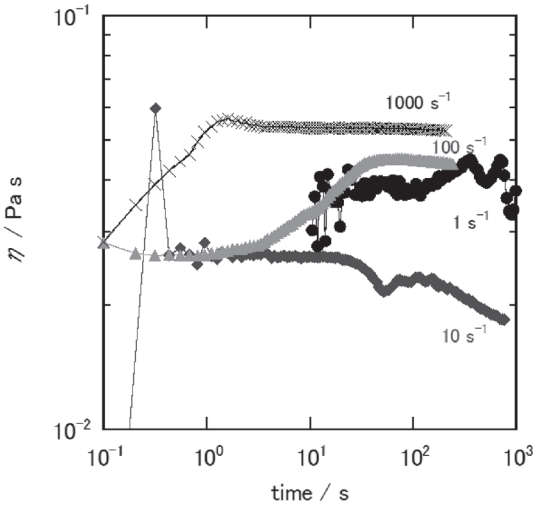

Figure 9. Relationship between viscosity and shear time at fixed shear rates. Shear rates are 1, 10, 100, and 1,000 s^{-1}. The horizontal logarithmic axis shows shear time, and the vertical logarithmic axis shows viscosity.

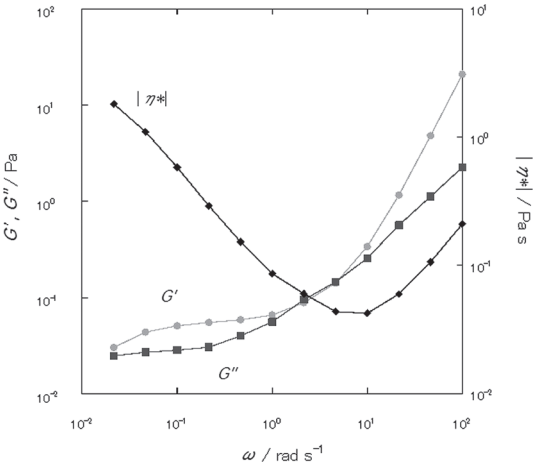

Figure 8. Frequency dependence of the storage modulus G', the loss modulus G'', and the absolute value of the complex viscosity $|\eta^*|$ for suspension of barium sulfate contrast agent (BarytesterA240, 200 w/v%).

these forces are weak and that the inter-particle network is fragile.

The dynamic rheologic measurements are shown in Figure 8. The absolute value of the complex viscosity $|\eta^*|$ is clearly dependent upon the angular frequency. Because the magnitude of G' was larger than G'' in the major part of the angular frequency range, this barium sulfate suspension may indicates the elastic response. However, the G' and G'' curves intersected at the range of 1 to 10 rads^{-1}. In this range of angular frequency, because the viscous response potentially represented by G'' slightly exceeds the elastic response represented by G', this barium sulfate suspension may indicates the viscous response. The relationship between viscosity and shear time at fixed shear rates is shown in Figure 9. The viscosity at a shear rate 10 s^{-1} decreased over time and exhibited thixotropic behavior. The shear rate of 10 s^{-1} corresponds to the range in shear rate that occurs during chewing and swallowing (Table 5)[11]. It is thought that the viscosity of the barium sulfate contrast suspension decreases in the act of swallowing, causing it to be easier to swallow. One reason for this thixotropic behavior is a potential deformation in the inter-particle network. The vis-

Table 5. Typical shear rates of some familiar materials and processes (Ref. 11).

Situation	Range of shear rates [s^{-1}]	Application
Draining under gravity	10^{-1}–10^{1}	Painting and coating
Extruders	10^{0}–10^{2}	Polymer
Chewing and swallowing	10^{1}–10^{2}	Foods
Dip coating	10^{1}–10^{2}	Paints, confectionery
Mixing and stirring	10^{1}–10^{3}	Manufacturing liquids
Spraying and brushing	10^{3}–10^{4}	Spray-drying, painting

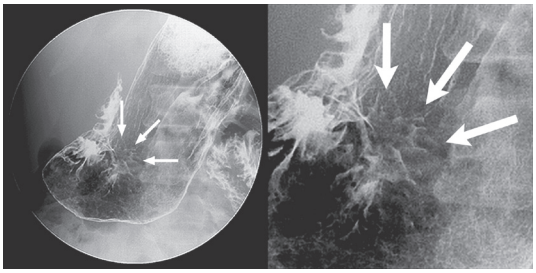

Figure 10. Double-contrast images in the right anterior oblique supine position. The IIc type early gastric cancer (arrows) with irregularly shaped erosion, which is barium-coated white area, is seen at the lesser curvature of the gastric angle. When filled with barium suspension, depressed lesions such as IIc type early gastric cancer appear as barium collection on the dependent gastric wall.

cosity at other shear rates (1, 100, and 1,000 s^{-1}) increased over time, and the sample became more dilatant. Therefore, the coating property of the gastric mucosa by the dilatant effect is maintained in the resting state, and also with a change in body position from the supine to the prone position and/or inverse change. The dilatant behavior is potentially caused by functional loss of excipients such as dispersant. Another reason for this behavior is thought that the transition from a two- to three-dimensional spatial arrangement of the particles at higher shear rate and the depletion forces caused by bimodal suspensions[12-14] ; however, further studies are needed to confirm this.

The double-contrast image of IIc type early gastric cancer, which is present on the lesser curvature of the gastric angle, is shown in Figure 6. In the Japanese classification system for early gastric cancer, the superficial type of early gastric cancers divided into three types as follows ; type IIa (elevated), IIb (flat), or IIc (depressed) lesions[16]. At the portion of gastric angle, it may be difficult to coat gastric mucosa well with barium sulfate suspension because the mid lesser curvature such as gastric angle is a vertical structure in the supine position. However, if the HD product suspension viscosity is adequately controlled, the fine mucosal detail included early gastric cancer may be clearly visible by dilatant behavior (Fig. 10).

4. Conclusion

Recent HD products have been developed and used in gastric cancer screening in many medical institutions. The high-density, low-viscosity barium suspension has been specifically created to maximize the identification of fine mucosal detail by use of a double-contrast imaging method. For achieving a high barium density with low viscosity, a barium sulfate suspension was formulated with a significant portion of large particles, increasing the potential packing density and lowering the viscosity by decreasing the relative amount of water adsorbed onto the surface of the barium-sulfate particles. We confirmed that HD products on the market contain fine particles and coarse particles. The coarse

particles were composed of large particles reaching approximately 30 μm. When well prepared, the HD product suspensions maintain an adequate viscosity over time. However, aspiration of the HD product suspension has been reported occasionally because the low viscosity facilitates swallowing[15]. No drug is without risk. It is necessary to have precise information concerning available HD products, including the particle size distribution, viscosity, concentration of barium sulfate, and functional excipients, because all of these factors are inter-related.

Acknowledgments

The authors are particularly grateful to associate professor Mitsumasa Kimata (Department of Chemistry and Chemical Engineering, Yamagata University) and associate professor Masataka Sugimoto (Department of Polymer Science and Engineering, Yamagata University) for help in measurements of particle size and rheological properties.

References

1) Thomsen, H.S., Webb, J.A.W. : Contrast media safety issue and ESUR guideline, 2nd revised edition, Springer, Berlin Heidelberg, 2006, 223-226
2) Tubono, Y., Hisamichi, S. : Screening for gastric cancer in Japan, Gastric cancer, **3**, 9-18, 2000
3) Nagahama, R., Nakashima, H., Yamamoto, T., Yoshida, M. : Diagnostic imaging for early gastric cancer-method and accuracy of screening by radiography, Stomach and Intestine, **44**, 563-570, 2009 (in Japanese)
4) Baert, A.L. : Encyclopedia of Diagnostic Imaging, Springer-Verlag, New York, 2008, 485-490
5) Gelfand, D.W. : High density, low viscosity barium for fine mucosal detail on double-contrast upper gastrointestinal examinations, Am. J. Roentgenol., **130**, 831-833, 1978
6) Low, V.H., Levine, M.S., Rubesin, S.E., Laufer, I., Herlinger, H. : Diagnosis of gastric carcinoma sensitivity of double-contrast barium studies, Am. J. Roentgenol., **162**, 329-334, 1994
7) Cullity, B.D. : Elements of X-ray diffraction, Addison-wesley publishing company, Inc., USA, 1956, 78-103
8) Gregory, J. : Particles in water, CRC press, Boca Raton, 2006, 9-46
9) Coulson, J.M., Richardson, J.F. : Chemical engineering vol.2 5th edition : particle technology and separation processes, Butterworth-Heinemann, Oxford, 2002, 11-17
10) Schramm, G. : A practical approach to rheology and rheometry 2nd edition, Gebrueder Haake, Karlsruhe, 2000, 119-141
11) Barnes, H.A., Hutton, J.F., Walter, K. : An Introduction to Rheology, Elsevier, Amsterdam, 1989, 12-15
12) Barnes, H.A. : Shear-thickening ("Dilatancy") in suspensions of nonaggregating solid sarticles dispersed in newtonian liquids, J. Rheol., **33**, 329-366, 1989
13) Lootens, D., van Damme, H., Hémar, Y., Hébraud, P. : Dilatant flow of concentrated suspensions of rough particles, Phys. Rev. Lett., **95**, 268302, 2005
14) Lionberger, R.A. : Viscosity of bimodal and polydisperse colloidal suspensions, Phys. Rev. E Stat. Nonlin. Soft Matter Phys., **65**, 061408, 2002
15) Ohkuma, R., Uematsu, M., Fujishima, I., Mukai, A. : Aspiration of barium contrast medium at gastric mass survey : investigation of aspiration cases encounterd in upper gastrointestinal radiographic contrast study and its prevention, Jpn. J. Rehabil. Med., **39**, 180-185, 2002 (in Japanese)
16) Ichikawa, H., Yamada, T., Horikoshi, H., Doi, H., Matsue, H., Tobayashi, K., Sasagawa, M., Higa, A. : X-ray diagnosis of early gastric cancer, Jpn. J. Clin. Oncol., **1**, 1-18, 1970